Human erythroid differentiation requires VDAC1-mediated mitochondrial clearance

Martina Moras,[1,2,3] Claude Hattab,[1,2,3] Pedro Gonzalez-Menendez,[3,4] Claudio M. Fader,[5,6] Michael Dussiot,[3,7] Jerome Larghero,[8] Caroline Le Van Kim,[1,2,3] Sandrina Kinet,[3,4] Naomi Taylor,[3,4,9] Sophie D. Lefevre[1,2,3#] and Mariano A. Ostuni[1,2,3#]

[1]Université de Paris, UMR_S1134, BIGR, Inserm, Paris, France; [2]Institut National de Transfusion Sanguine, Paris, France; [3]Laboratoire d'Excellence GR-Ex, Paris, France; [4]Institut de Génétique Moléculaire de Montpellier, Université de Montpellier, CNRS, Montpellier, France; [5]Laboratorio de Biología Celular y Molecular, Instituto de Histología y Embriología (IHEM), Universidad Nacional de Cuyo, CONICET, Mendoza, Argentina; [6]Facultad de Odontología, Universidad Nacional de Cuyo, Mendoza, Argentina; [7]Université de Paris, UMR_S1163, Laboratory of Cellular and Molecular Mechanisms of Hematological Disorders and Therapeutical Implication, INSERM, Paris, France; [8]AP-HP, Hôpital Saint-Louis, Unité de Thérapie Cellulaire, Paris, France and [9]Pediatric Oncology Branch, Center for Cancer Research (CCR), National Cancer Institute (NCI), National Institutes of Health (NIH), Bethesda, MD, USA

[#]SDL and MAO contributed equally as co-senior authors

 doi:10.3324/haematol.2020.257121

Received: April 29, 2020.

Accepted: December 21, 2020.

Pre-published: January 7, 2021.

Correspondence: *MARIANO A. OSTUNI* - mariano.ostuni@inserm.fr

SOPHIE D. LEFEVRE - sophie.lefevre@inserm.fr

Human erythroid differentiation requires VDAC1-mediated mitochondrial clearance

Martina Moras[1,2,3], Claude Hattab[1,2,3], Pedro Gonzalez-Menendez[3,4], Claudio M. Fader[5,6], Michael Dussiot[7], Jerome Larghero[8], Caroline Le Van Kim[1,2,3], Sandrina Kinet[3,4], Naomi Taylor[3,4,9], Sophie D. Lefevre[1,2,3*#], Mariano A. Ostuni[1,2,3*#]

Running Head: **VDAC-driven mitophagy in human erythropoiesis**

corresponding authors
Mariano A. OSTUNI and Sophie D. LEFEVRE
UMR_S1134 Biologie Intégrée du Globule Rouge
6, rue Alexandre Cabanel
75739 Paris cedex 15, FRANCE
Email address: mariano.ostuni@inserm.fr; sophie.lefevre@inserm.fr
Phone: +33 1 44 49 31 35
Fax: +33 1 43 06 50 19

Supplementary Methods

Purification and culture of CD34$^+$ cells

Cord blood mononuclear cells (CBMCs) from healthy donors were used in this study. Umbilical cord blood that cannot be qualified for the use in patients was obtained from the center for biological resources from Saint-Louis Hospital Cord Blood Bank registered to the French Ministry of Research under number AC-2016-2756, and to the French Normalization Agency under number 201/51848.1. This study was approved and conducted according to institutional ethical guidelines of the National Institute for Blood Transfusion (N°2019-1, INTS, Paris, France). It was also approved by the Ethics committee of INSPIRE program (Horizon 2020 grant agreement 665850). All procedures were carried out in accordance to the Declaration of Helsinki. Written informed consent was given by the donors. PBMCs were separated from whole blood using Ficoll (GE healthcare) and CD34$^+$ cells were purified from cord blood by positive selection using the magnetic-activated cell sorting magnetic beads system (Miltenyi Biotec), according to the manufacturer's instructions.

CD34$^+$ cells were cultured in Iscove's Modified Dulbecco's Medium (Invitrogen), 2% human peripheral blood plasma (Stem Cell Technologies), 3% human AB serum (Sigma Aldrich), 15% BIT 9500 Serum Substitute (Stem Cell Technologies) and 3 IU/mL heparin (Sigma Aldrich). For the expansion phase (day -4 to day 0), cells were seeded at a concentration of 10^5 cells/mL in culture medium supplemented with 25 ng/mL stem cell factor (SCF, Miltenyi Biotec), 10 ng/mL IL-

3 (Miltenyi Biotec) and 10 ng/mL IL-6 (Miltenyi Biotec). In the phase I (day 0 to day 6), medium was supplemented with 10 ng/mL SCF, 1 ng/mL IL-3 (Miltenyi Biotec) and 3 IU/mL erythropoietin. IL- 6 was omitted from the culture medium. In the phase II (day 7 to day 10), IL-3 was omitted from the culture medium. In the phase III (that lasted until day 17) SCF was omitted.

VDAC1 silencing plasmid and lentiviral production

Lentiviruses particles were produced by co-transfection of HEK293T cells with the plasmids MISSION® pLKO.1-puro Non-Target shRNA Control Plasmid DNA or shVDAC1 (TRCN0000297481, responding sequence, 5′-GCAGTTGGCTACAAGACTGAT-3′) with the 714bp EGFP sequence that was inserted in place of the puromycin gene at the unique BamHI and KpnI restriction sites, together with the helper plasmids Δ8.9 and VSV-G in HBS buffer (454 µM NaCl, 23 mM Na_2HPO_4, 28 mM KCl, 216 mM dextrose, pH = 7.05) and 132 mM $CaCl_2$. On the following day, the medium was replaced with DMEM without serum, and the cells were cultured for 1 day before the supernatant containing viruses was collected. Viruses were concentrated by OVN centrifugation at 4000 rpm at 4 °C.

Cell Culture and small interference (siRNA) or short hairpin (shRNA) transfection

K562 cells were maintained in RMPI 1640 medium (ThermoFischer, France), supplemented with 10 % fetal calf serum and 1 % antibiotics penicillin-streptomycin. The cells were incubated at 37°C in a humidified atmosphere with 5 % CO_2 and 95 % air. K562 cells in exponential phase were transfected by electroporation (Amaxa, Nucleofector Kit V, France) with MISSION® pLKO.1-puro plasmids. shSCR-K562 and shVDAC1-K562 stable cell lines were created using puromycin selection. For mitophagy induction, cells were challenged with 50 µM CCCP for 4 hours at 37°C. Cells were then transfected with one of the following small-interfering (si)RNA duplexes (ThermoFisher scientific, France): Ambion® Silencer® Negative Control #5 siRNA (AM4642), VDAC1 siRNA (s14769), PINK1 siRNAn°1 (s35166) and PINK1 siRNA n°2 (s35168).

Antibodies and dyes

The following antibodies (Ab) and corresponding dilution were used for Western blotting: monoclonal mouse anti-VDAC1 Ab (Santa Cruz, sc-390996, 1:500), rabbit anti-MAP LC3B Ab (Sigma Aldrich, L7543, 1:200), rabbit anti-p62 Ab (GeneTex, GTX100685, 1:1,000), rabbit anti-PINK1 (GeneTex, GTX107851, 1:1000),), rabbit anti-BNIP3L (GeneTex, GTX111876, 1:1000), mouse anti-TOM40 Ab (Santa Cruz, sc-365467, 1:1000), HRP-coupled anti-rabbit Ab (Jackson, 111-035-144, 1:5000), HRP-coupled anti-mouse (Jackson, 115-035-003, 1:5000), HRP-coupled anti-actin Ab (Cell signaling, 13E5, 1:3,000). For immunostaining: mouse anti-TOM22 (Abcam,

ab57523, 20 µg/mL), rabbit anti-MAP LC3B Ab (Sigma Aldrich, L7543, 1:100), Alexa Fluor 568 Goat anti–rabbit IgG Ab and Alexa Fluor 633 Goat anti–mouse IgG Ab (Thermo Fisher Scientific, 1:200). PE-conjugated mouse anti-human Band3 (IBGRL, 9439PE BRIC 6, 1:50), PE-Cy7-conjugated mouse anti-human CD235a (BD Pharmigen™, 563666, 1:20), APC-H7-conjugated mouse anti-human CD49d (BD Pharmigen™, 656153, 1:10) were used for flow cytometry. Mitotracker (MitoFluor Red 589 (M-22424), 250 nM or Mitotracker Deep Red (M22426), 50 nM) were used for mitochondria staining. Hoechst 34580 (BD Pharmingen™, 1 µg/mL) was used for enucleation assay in imaging flow cytometry and Hoechst 33342 (BD Pharmingen™, 1 µg/mL) was used for flow cytometry-based analysis of erythroid differentiation. PE-coupled Annexin V (BD Pharmingen™, 1:20) were used for viability assay in flow cytometry. 7-Aminoactinomycin D (7AAD, Thermo Fisher Scientific, 1:200) was used as viability staining in flow cytometry.

MGG-based identification of erythroblasts stage

10^5 of total and sorted cells according to α4-integrin and Band3 surface expression as described by Hu et al. 2013 (1), were cytospun using the Thermo Scientific Shandon 4 Cytospin to validate the gates. The slides were stained with May-Grunwald (Sigma Aldrich, MG500) solution for 5 min, with May-Grunwald solution diluted by half for other 5 min, and subsequently stained with Giemsa solution (Sigma Aldrich, GS500) diluted 10 times for 15 min. Cells were imaged using a Nikon Eclipse Ti-S inverted microscope with a 40x/0.6 Plan Fluor objective.

Apoptosis assay

Cells were washed in PBS and then resuspended in 100 µL of Annexin Buffer containing PE-coupled Annexin V. After 15 min of incubation at room temperature in the dark, 400 µL of Annexin buffer was added. Viability was assessed by flow cytometry.

Seahorse analysis

Oxygen consumption rate (OCR) was measured using the Seahorse XFe-96 Extracellular Flux Analyzer (Agilent). The day before the analysis the plate was calibrated with 200 µl of OVN calibration buffer per well at 37 °C. The following day the plate was coated with 100 µg/mL poly-D-lysine for 1h at RT. $3x10^5$ cells were added in each well in XF media (non-buffered DMEM containing 10 mM glucose and 2 mM L-glutamine) and incubated at 37 °C without CO_2. The Mito Stress test was performed using 1 µM oligomycin, 1 µM FCCP, 100 nM rotenone and 1 µM antimycin A. After each addition inhibitor at least 3 sequential measurements were taken. Analysis of OCR data were performed using Wave software. As OCR values depend on the mitochondrial number, data were normalized using MFI values of Mitotracker Deep Red previously measured by flow cytometry.

SDS-PAGE and Immunoblotting

Whole-cell lysates of cultured cells were prepared buffer 10 mM Tris-HCl pH 6.8, 1 mM EDTA, 10% SDS, containing 1X cOmplete™ protease cocktail inhibitor (Roche). After sonication, cells were frozen for at least 1 h. Protein quantification was performed by Pierce™ BCA Protein Assay Kit (Thermo Fisher Scientific) and 30 µg of proteins were separated using NuPAGE® 4-12% Bis-Tris gels. After proteins transfer to a nitrocellulose membrane using Trans-Blot Turbo Transfer System (BioRad), immunoblotting was done with primary antibody overnight at 4 °C. Proteins of interest were revealed using HRP-conjugated secondary antibodies and the Enhanced Chemiluminescence kit (Perkin Elmer). Images were acquired by ChemiDoc™ Imaging Systems (Bio-Rad) and bands intensity were quantified with Image Lab software (Bio-Rad).

Quantitative real time qPCR

Total RNA was extracted using RNeasy kit (Qiagen) and quantified by NanoDrop 2000c (Thermo Scientific™). Reverse transcription of 2 µg of total RNA was performed using MultiscribeTM Reverse Transcriptase (Applied Biosystems) and gene expression assays were performed using QuantiNova SYBR Green RT-PCR Kit or QuantiNova Probe RT-PCR Kit (Qiagen). Primers used for assays were obtained from Eurofins MWG Operon. VDAC1 Fw 5'-AGCTGACCTTCGATTCATCCTTC-3' Rv 5'-TAATGTGCTCCCGCTTGTACC-3', VDAC2 Fw 5'-AGTCTTGCAGTGGCGTGG-3' Rv 5'-TGGTCTCCAAGGTCCCAGTA-3', VDAC3 Fw 5'-CAGATGAGTTTTGACACAGCCA-3' Rv 5'-TCCAAATTCAGTGCCATCGTTC-3', NIX Fw 5'-GCCGGCCTCAACAGTTC-3' Rv 5'- TGGCATTTGCGGAAAAGA-3'. Relative quantification of fold change was performed comparing Ct values from individual samples by applying the Pfaffl Method (2). Results were normalized for each of the samples by the expression of the TATA box binding protein (Prime Time® qPCR Assay, Hs.PT.58.19838260; Integrated DNA Technology).

Immunolabelling for confocal microscopy and imaging flow cytometry

Cells were fixed in 3% PFA and quenched with 50 mM NH_4Cl. Cells were permeabilized used 1% saponine/BSA (v/v in PBS) before staining overnight at 4 °C with primary antibodies. Cells were next incubated with AF546/AF647/AF633-conjugated Alexa secondary antibodies at RT for 1h in the dark. For confocal microscopy, $3x10^5$ cells were cytospun using Thermo Scientific Shandon 4 Cytospin and mounted with DAPI Fluoromount-G® (SouthernBiotech) before imaging with LSM 700 Laser Scanning Microscope (Zeiss) with a 63x/1.4 Oil Plan Apochromat objective. Zen and Fiji software were used to acquire images and process them, respectively. Colocalization tool from Imaris software (Oxford Instruments) was use for analyzing. After washing, 1 million cells were resuspended

in a total volume of 50 µl and image acquisition was performed. Samples were run on an Imagestream ISX mkII (Amnis Corp, Luminex, Seattle, WA) and a 60X magnification was used for all acquisitions. Data were acquired using the INSPIRE software (Amnis Corp) and analyzed using the IDEASTM software (Version 6.2 Amnis Corp). On average, 30,000-50,000 events were collected in all experiments. Single stain controls were run for each fluorochrome used and spectral compensation was performed. Cells were gated for single cell using the area and aspect ratio of the brightfield image, then gated for focused cells using the gradient RMS feature; GFP positive cells were selected. A TOM mask was created to study its colocalization with PINK and LC3. TOM, PINK and LC3 quantification was expressed as mean pixel intensity value (MPI), which is the intensity normalized to surface area of the mask for TOM compartment. Colocalization was performed on double positive population and was determined by the ratio of the MPI of PINK or LC3 to the MPI of TOM, or using the Bright Detail Similarity R3 feature (BDS), which is the log transformed Pearson's correlation coefficient of the localized bright spots with a radius of 3 pixels within TOM mask between TOM and PINK or TOM and LC3. The Modulation feature, which measures the intensity range of an image, normalized between 0 and 1, was determined for LC3 in the cytoplasm mask. Modulation formula is Max Pixel - Min Pixel / Max Pixel + Min Pixel. Each result is the pool of 3 experiments.

ATP measurement by luminometer

Intracellular ATP was measured by quantitative luminometry using firefly luciferase, which catalyzes the oxidation of luciferin in the presence of ATP to produce light. $3x10^5$ cells were frozen and resuspended in 150 µL of water. 5 µL of this lysate were added to 45 µL of a luminometry mix (RBC medium containing 0.01 µM luciferase, 0.2 mM luciferin, and 0.1 mg/mL of Coenzyme A), directly in the assay chamber of a custom-built luminometer as previously described (3), to determine the light intensity. Calibration of the luminometric signal was performed at the end of each measurement with ATP serial dilution from 1 µM to 16 µM.

Electron microscopy

After fixation with 2.5% glutaraldehyde, 10^6 erythroblasts (day 10 of differentiation) were post-fixed with osmium tetroxide 2% in cacodylate, pH 7.4, progressively dehydrated in acetone, and embedded in low-viscosity epoxy resin. 60-nm-thin sections were cut, mounted on copper grids, and stained with uranyl acetate and lead citrate. Sections were examined with a Zeiss EM900 electron microscope and archived with a CDD camera Gatan Orius CS1000.

Mitochondrial Morphology

As previously described (4), mitochondrial morphology was calculated from the Aspect Ratio, which is the ratio between the major and minor axis of the object considered as an ellipse. The result obtained determines the organelle length. These parameters, independent of the magnification of the image, have a minimum value of 1 corresponding to a circular shape of the mitochondria. Statistical tests were performed to compare the obtained images according to the different treatments. Mitochondria-ER contact sites were quantified following previously described protocols (5,6) adapted from (7)

ROS detection

Cells were stained with CellROX Deep Red Reagent (Thermo Fisher Scientific, C10422, 5 µM) for total ROS staining, 30 min at 37 °C. After washing, cells were subsequently analyzed by flow cytometry.

Mitochondrial membrane potential assay

Cells were stained with MitoTracker™ Red CMXRos (Thermo Fisher Scientific, M7512, 250 nM) 30 min at 37 °C. After washing, cells were subsequently analyzed by flow cytometry.

Statistical Analysis

Each experiment was repeated at least 3 times, with a satisfactory correlation between the results of individual experiments. Statistical analyses were performed using Prism 6 (Graph Pad Software). Data were evaluated using the unpaired t-test and all comparisons with a p value less than 0.05 ($p < 0.05$) were considered statistically significant. $p<0.0001$, $p<0.001$, $p<0.01$, and $p<0.05$ are indicated with four, three, two, or one star (s), respectively. The data are expressed as the mean ± the standard error of the mean (SEM).

References

1. Hu J, Liu J, Xue F, Halverson G, Reid M, Guo A, et al. Isolation and functional characterization of human erythroblasts at distinct stages: implications for understanding of normal and disordered erythropoiesis *in vivo*. Blood. 2013; 121(16):3246-53.
2. Pfaffl MW. A new mathematical model for relative quantification in real-time RT-PCR. Nucleic acids research. 2001; 29(9):e45.
3. Pafundo DE, Chara O, Faillace MP, Krumschnabel G, Schwarzbaum PJ. Kinetics of ATP release and cell volume regulation of hyposmotically challenged goldfish hepatocytes. American journal of physiology Regulatory, integrative and comparative physiology. 2008; 294(1):R220-33.

4. Vander Heiden MG, Chandel NS, Li XX, Schumacker PT, Colombini M, Thompson CB. Outer mitochondrial membrane permeability can regulate coupled respiration and cell survival. Proceedings of the National Academy of Sciences of the United States of America. 2000; 97(9):4666-71.

5. Modi S, López-Doménech G, Halff EF, Covill-Cooke C, Ivankovic D, Melandri D, et al. Miro clusters regulate ER-mitochondria contact sites and link cristae organization to the mitochondrial transport machinery. Nat Commun. 2019; 10(1):4399

6. Issop L, Fan J, Lee S, Rone MB, Basu K, Mui J, et al. Mitochondria-associated membrane formation in hormone-stimulated Leydig cell steroidogenesis: role of ATAD3. Endocrinology. 2015; 156(1):334-45.

7. Crowther RA, Amos LA, Finch JT, De Rosier DJ, Klug A. Three dimensional reconstructions of spherical viruses by fourier synthesis from electron micrographs. Nature; 226(5244):421-5.

Supplementary Figures

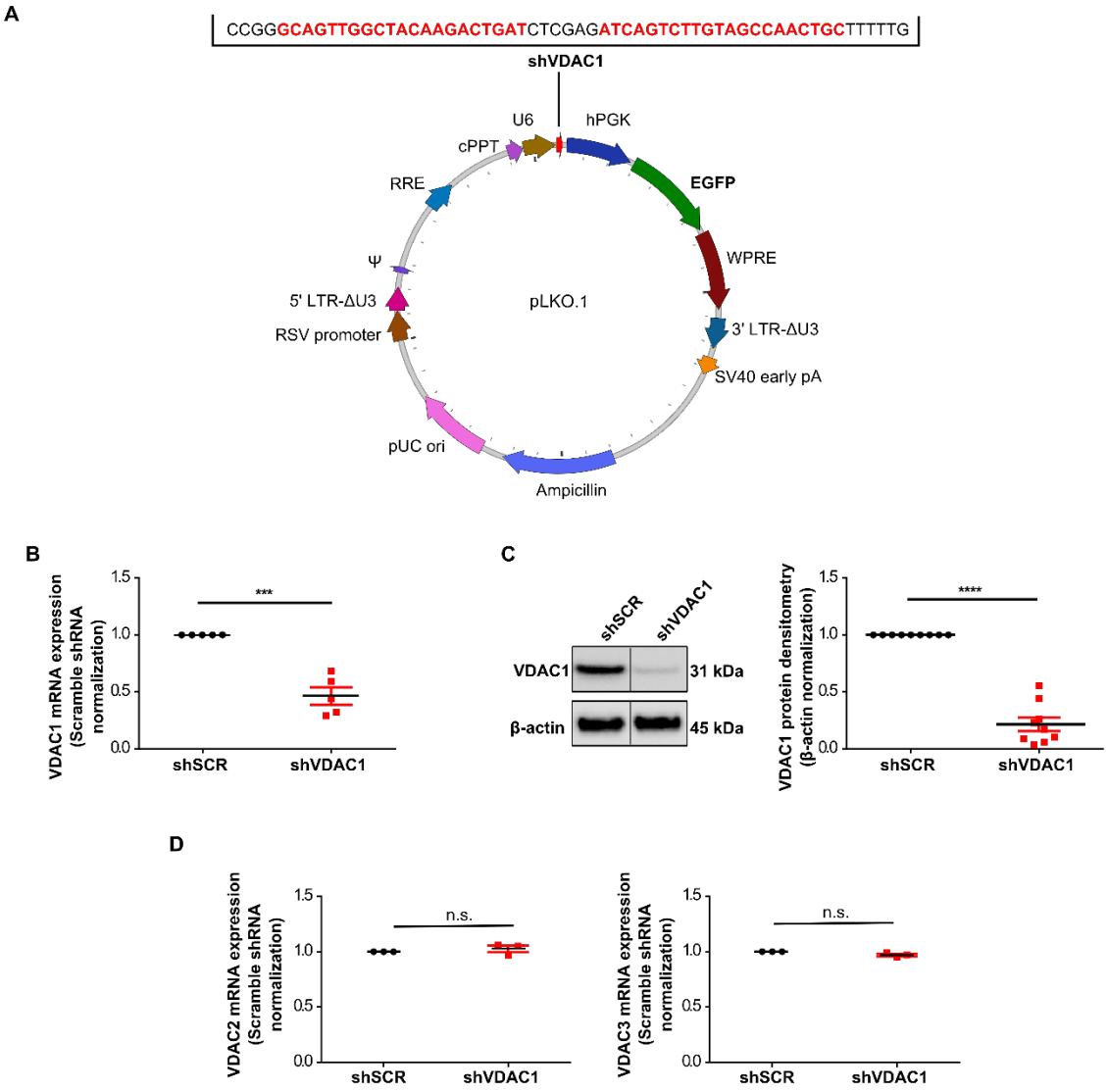

Figure S1. Downregulation of VDAC1 by a VDAC1-specific shRNA does not alter expression of VDAC2 or VDAC3 isoforms. (A) Map of the pLKO.1 vector showing the shVDAC1 insert sequence. (B) RT-qPCR (n = 5) and (C) Western Blot-based quantification (n = 9) of VDAC1 levels (day 10) (D) mRNA levels of VDAC2 and VDAC3 were evaluated in erythroblasts transduced with shSCR or shVDAC1 (n = 3). Levels in shSCR-transduced cells were arbitrarily set at "1". Representative data and mean levels ±S.E. are shown. ***p<0.001, ****p<0.0001.

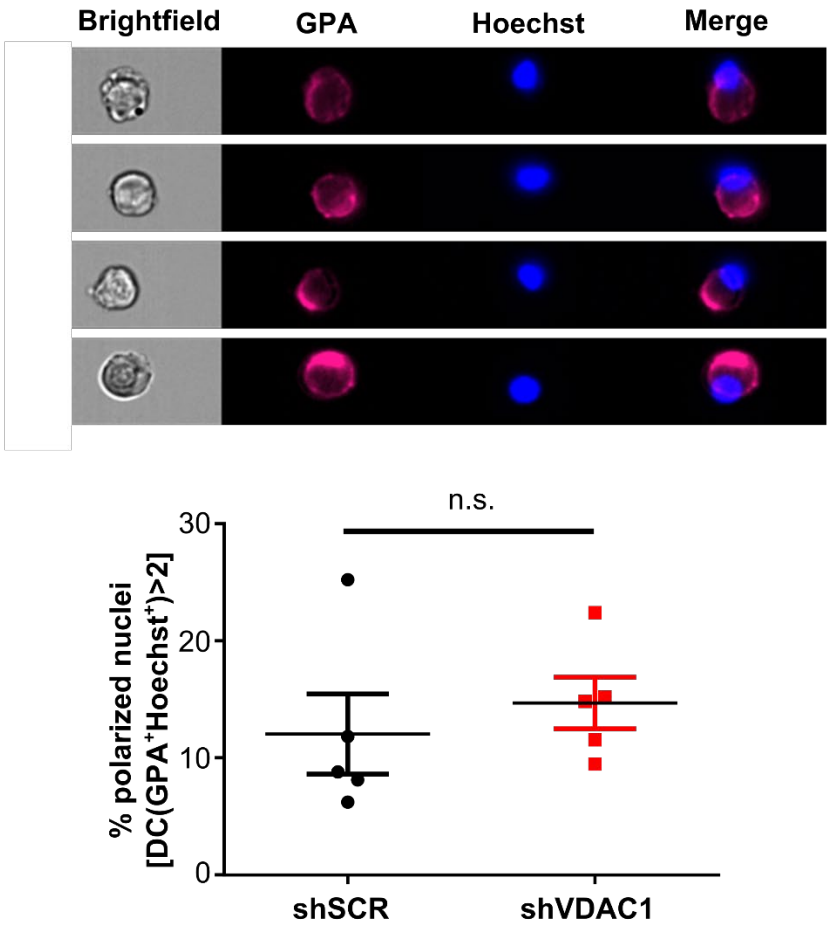

Figure S2. Downregulation of VDAC1 does not alter the polarization of the nuclei.

The presence of polarized nuclei was evaluated in FACS-purified orthochromatic erythroblasts 24 h post isolation by imaging flow cytometry. "Delta centroid GPA-Hoechst" (DC) with a threshold of 2 was arbitrary choose to discriminate polarized nuclei. Representative images (left) and quantification of polarized nuclei (right) in the different conditions are shown (n = 5).

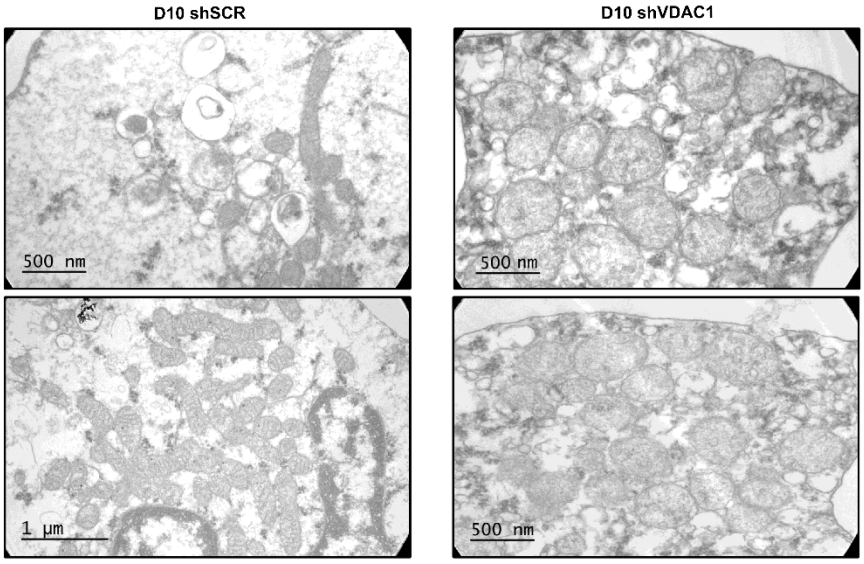

Figure S3. Mitochondria morphology is altered in erythroblasts following VDAC1 downregulation. Sample TEM images of erythroblasts at day 10 of differentiation.

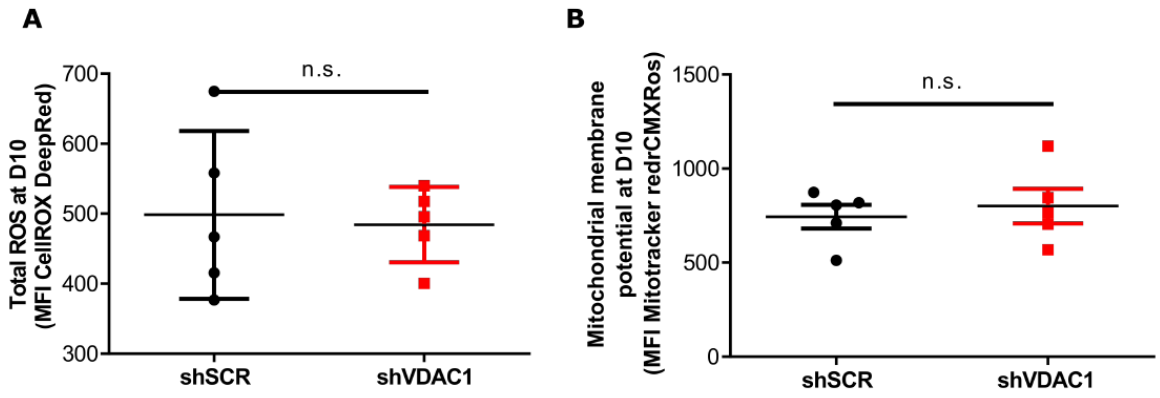

Figure S4. ROS production and mitochondrial membrane potential are not affected by downregulation of VDAC1. (A) Total ROS production quantification by flow cytometry (CellROX Deep Red Reagent) (n = 5) and (B) mitochondrial membrane potential (MitoTracker™ Red CMXRos) quantification measured at day 10 of differentiation (n = 5) and MFI of shSCR (black dots) and shVDAC1 (red dots) are presented.

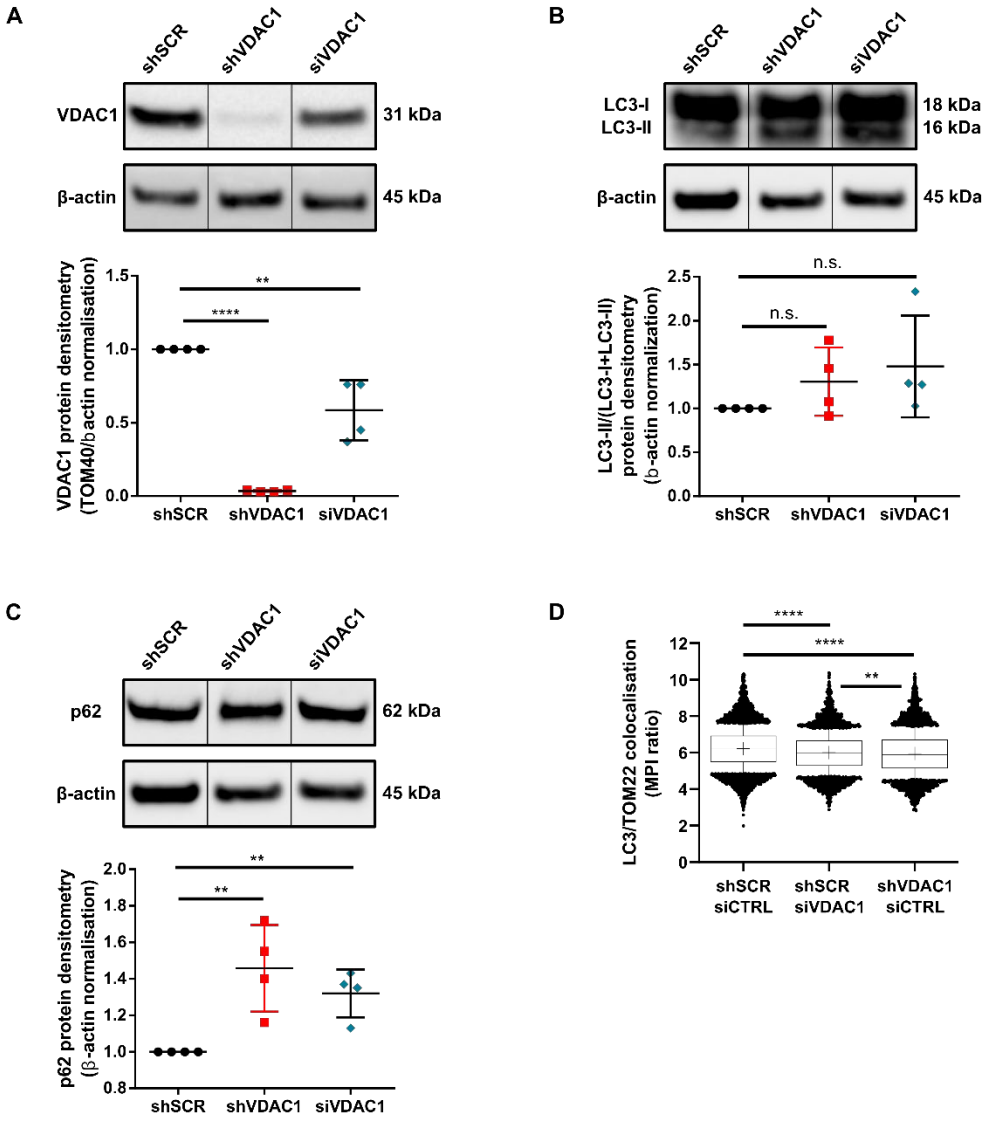

Figure S5. Lack of phagophore recruitment in shVDAC1-K562 cell line. (A) VDAC1 protein levels were evaluated by immunoblot in shSCR-K562, shVDAC1-K562 cell lines and VDAC1 siRNA-transfected shSCR-K562 cells and normalized to the quantity of mitochondria (TOM40) on total number of cell (β-actin). Levels in control cells were arbitrarily set at "1" (n = 4). (B) LC3-I and LC3-II levels were evaluated by immunoblots. LC3-II/total LC3 levels were normalized to β-actin with levels in control cells arbitrarily set at "1" (n = 4). (C) p62 levels were assessed by immunoblots and normalized to β-actin with levels in control cells arbitrarily set at "1" (n = 4). (D) LC3/TOM22 colocalization (MPI ratio) assessed by imaging flow cytometry of shSCR-K562 cells transduced or not with VDAC1 siRNA and shVDAC1-K562 cells (n =3). **p<0.01, ****p<0.0001

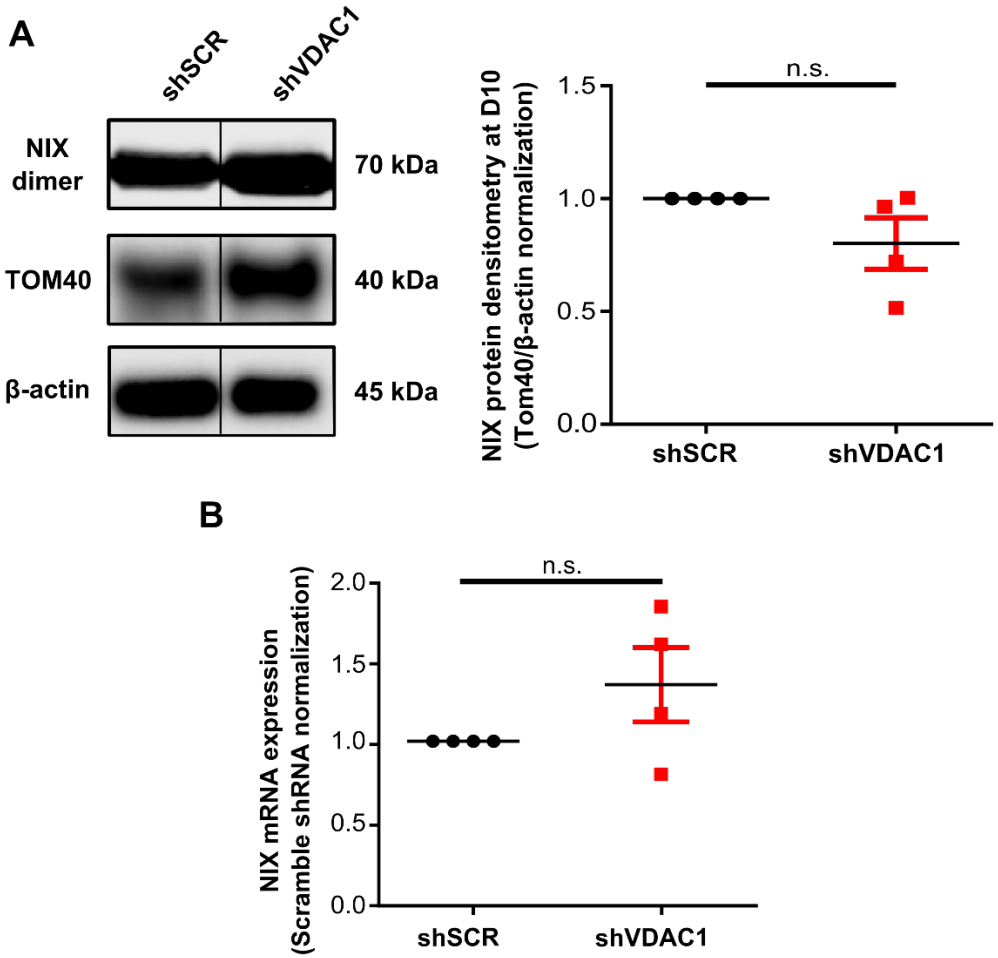

Figure S6. NIX levels are not affected by downregulation of VDAC1. (A) The presence of NIX dimers was assessed by Western Blot at day 10 of differentiation (n = 4) and normalized to the quantity of mitochondria (TOM40) on total number of cell (β-actin). (B) NIX mRNA levels were evaluated by RT-qPCR in sorted polychromatic cells and levels in shSCR-transduced cells were arbitrarily set at "1" (n = 4).